Subdominant Modes in Zonal-Flow-Regulated Turbulence

K. D. Makwana,[*] P. W. Terry, and M. J. Pueschel

Department of Physics, University of Wisconsin-Madison, Madison, Wisconsin 53706, USA

D. R. Hatch

Institute for Fusion Studies, University of Texas at Austin, Austin, Texas 78712, USA

From numerical solutions of a gyrokinetic model for ion temperature gradient turbulence it is shown that nonlinear coupling is dominated by three-wave interactions that include spectral components of the zonal flow and damped subdominant modes. Zonal flows dissipate very little energy injected by the instability, but facilitate its transfer from the unstable mode to dissipative subdominant modes, in part due to the small frequency sum of such triplets. Although energy is transferred to higher wave numbers, consistent with shearing, a large fraction is transferred to damped subdominant modes within the instability range. This is a new aspect of regulation of turbulence by zonal flows.

Turbulence driven by ion gyroradius-scale microinstabilities limits confinement in magnetically confined fusion plasmas [1]. The turbulence saturates when the rate of energy injection by the instability is balanced by the rate of energy dissipation. In the traditional view, dissipation arises at small scales. However, plasma instabilities represent one root (or a few) of dispersion relations that typically have many other stable roots at any given wave number of the spectrum. These modes dissipate energy at large scales, within the wave number range of the instability. They are excited to finite amplitude by three-wave interactions that couple unstable and stable modes of a wave number triplet [2]. Such modes have been shown to be the dominant saturation mechanism in a variety of fusion plasma turbulence models [3]. The energy dissipation rate in the wave number range of the instability is comparable to the instability energy injection rate, creating a saturation process that is fundamentally different from a cascade to collisionally dissipative, large wave numbers.

Ion temperature gradient (ITG) driven turbulence, an important contributor to ion heat transport in tokamaks, is regulated by zonal flows, i.e., self-generated, toroidally and poloidally symmetric, radially sheared $\mathbf{E} \times \mathbf{B}$ flows [4]. Zonal flows are driven to high amplitude in ITG turbulence as a result of turbulent interactions [5,6]. Conventionally, the regulation of ITG turbulence by zonal flows is explained by zonal flow shearing [6]: zonal flows shear apart turbulent eddies, causing enhanced energy transfer to small dissipative scales and saturating ITG turbulence. Given that stable modes have also been found to be important in the saturation of ITG in both fluid and gyrokinetic analyses [7], it is crucial to investigate the role of stable modes in zonal-flow-regulated ITG turbulence.

In Ref. [8], analysis of a simple two-field fluid ITG model uncovered evidence for a different mechanism of zonal flow regulation. Zonal flows provide a high-efficiency energy-transfer channel from the unstable mode to a large-scale stable mode that saturates the turbulence. With efficient transfer, the turbulence level is low. Because the zonal flow absorbs only a small fraction of the energy transferred, it acts as a catalyst. However, the fluid model treats the enhanced nonlinear excitation of zonal flows artificially, includes only one stable mode, and its modeling of dissipation has only crude collisional diffusivities with no kinetic resonance effects. Thus, the essential analysis of the role of stable modes in zonal flow regulation using gyrokinetics [9,10], which overcomes the deficiencies of the fluid model, is given here.

We use the gyrokinetic code GENE [11], developing diagnostics that trace energy transfer between zonal flows, the unstable mode, and stable modes. These measure the partition of energy flow in the joint space of perpendicular wave number and the phase space of parallel motion spanned by stable modes. We probe the efficiency of energy transfer channels by measuring nonlinear triplet correlation times and amplitude dependence. GENE describes plasma dynamics in terms of the modified perturbed ion distribution function $g(k_x, k_y, z, v_\parallel, \mu, t)$ (see Ref. [12]). Here the radial and binormal wave numbers are denoted by k_x and k_y, normalized to the ion sound gyroradius ρ_s. Also, z is the equilibrium magnetic-field-line-following coordinate, $v_\parallel$ is the velocity in z direction, μ is the magnetic moment, and t is time. We simulate Cyclone base case parameters with adiabatic electrons and only electrostatic perturbations [13], using resolutions of $(128,16,16,32,8)$ for $(k_x, k_y, z, v_\parallel, \mu)$.

To study the energy transfer that underpins saturation, we look at the free energy (see Eqs. (5) and (10) of Ref. [14])

$$E \equiv \mathrm{Re}\left[\sum_k \int \hat{J}\pi B_0 dz dv_\parallel d\mu \frac{n_0 T_0}{F_0}\left(g_k^* + \frac{qF_0}{T_0}\bar{\phi}_k^*\right)g_k\right],$$

(1)

referred to as the "energy" from here on. Here, $\hat{J}$ is the normalized Jacobian, B_0 is the equilibrium magnetic field, F_0 is the background Maxwellian distribution function of the plasma, g_k is g at (Fourier) wave number $k = (k_x, k_y)$; n_0, T_0, and q are the background density, temperature, and charge, respectively; and $\bar{\phi}$ is the gyroaveraged electrostatic potential. The evolution equation for the energy at a particular Fourier wave number, $(dE_k/dt) = Q_k + C_k + R_k + (dE_k/dt)|_{\mathrm{NL}}$, follows from the gyrokinetic equation. Here, Q_k is proportional to the heat flux and provides the gradient drive, whereas C_k represents dissipation. We use artificial hyperdiffusion for C_k [12]. Expressions for these quantities can be found in Ref. [15]. These two terms are responsible for net energy injection into or dissipation out of the system. Unlike Q_k and C_k which are symmetric in k, R_k is a linear term depending on the gradient and curvature drifts, which is antisymmetric in k, i.e., $R_k = -R_{-k}$. Considering energy dynamics for a pair of k and $-k$ doubles Q_k and C_k while eliminating R_k; hence, we ignore R_k. The term $(dE_k/dt)|_{\mathrm{NL}}$ represents conservative energy transfer between wave numbers via nonlinear three-wave interaction. It is given by

$$\left.\frac{dE_k}{dt}\right|_{\mathrm{NL}} = \mathrm{Re}\left\{\sum_{k'} \int dz dv_\parallel d\mu \hat{J}\pi B_0(k' \times \hat{z} \cdot k)\right.$$
$$\left. \times\left[\frac{n_0 T_0}{F_0}g_k^*\bar{\phi}_{k-k'}g_{k'} - qn_0\bar{\phi}_k^*\bar{\phi}_{k'}g_{k-k'}\right]\right\}. \quad (2)$$

The effect of zonal flows on fluctuation amplitudes is well known. With Eq. (2) we quantify their effect on energy transfer rates. We separate the rhs into interactions that include a zonal wave number and those that do not. Zonal wave numbers have $k_y = 0$. Restricting the sum over k' to terms with either $k_y' = 0$ or $k_y - k_y' = 0$, one is calculating three-wave interactions that include a zonal wave number in the drive of nonzonal wave number k. Conversely, restricting the sum over k' to exclude these wave numbers provides coupling to nonzonal wave numbers. We normalize the coupling rates to the energy, $\gamma_{\mathrm{NL}} \equiv (1/E_k)(dE_k/dt|_{\mathrm{NL}})$, looking at the most energetic wave number, $k = (0, 0.25)$, in two cases. In the first case, zonal flows are artificially suppressed by zeroing the flux-surface-averaged electrostatic potential at every time step. On time average, the normalized coupling rate with zonal wave numbers (magnitude of -0.02) is very small compared to the normalized coupling rate with nonzonal wave numbers (-0.09). We still get a nonzero zonal coupling because only $\bar{\phi}(k_y = 0, k_z = 0)$ is made zero, whereas $g(k_y = 0, k_z = 0)$ is left unchanged. In the other case, when the zonal potential is allowed to evolve self-consistently; the normalized coupling

with zonal wave numbers is strong (-0.18) compared to the normalized nonzonal coupling (-0.075).

The change in relative coupling between zonal and nonzonal transfer channels indicates that transfer to zonal wave numbers is *relatively* stronger when the zonal flow is not suppressed. While the selection for zonal wave numbers encompasses many moments of the distribution (zonal flow, zonal pressure, etc.), the fact that a deletion of zonal flow causes drastic changes indicates that it is the coupling to zonal flows that drives the strong coupling with zonal wave numbers. Although it is possible that deleting other zonal moments (density, pressure, etc.) could also lead to significant changes [16], explicit measurements in the fluid model [8] show that energy transfer is dominated by zonal flows relative to zonal pressure.

To measure stable mode activity among the modes spanning z, $v_\parallel$, and μ for each k, we use proper orthogonal decomposition (POD) [15]. Under POD, the distribution function at k becomes $g_k(z, v_\parallel, \mu, t) = \sum_n \psi_k^{(n)}(z, v_\parallel, \mu) \times \beta_k^{(n)}\pi_k^{(n)}(t)$. Here, $\psi_k^{(n)}(z, v_\parallel, \mu)$ is the nth POD mode, $\beta_k^{(n)}$ is its singular value, and $\pi_k^{(n)}(t)$ is its time-dependent coefficient. These modes are useful for energy analysis because they are orthogonal under an inner product $\int dz dv_\parallel d\mu(1/F_0)\pi B_0\hat{J}(z)\psi_k^{*(m)}\psi_k^{(n)} = \delta_{m,n}$. However, the electrostatic potential modes $\bar{\phi}^{(m)}$ derived from POD modes $\psi^{(m)}$ are nonorthogonal. Substituting the POD in the energy expression (Eq. (1)), we get one term proportional to $\sum_n|\beta^{(n)}\pi^{(n)}|^2$ from the orthogonal POD modes and another term from the nonorthogonal potential modes. However, the nonorthogonal term is much smaller than the orthogonal term [less than 15% for $k = (0, 0.25)$]. Hence, we ignore this nonorthogonal contribution and define the energy of a POD mode as $E_k^{(n)} \equiv |\beta^{(n)}\pi^{(n)}|^2$.

The energy dynamics of a POD mode is derived by multiplying the gyrokinetic equation by a POD mode and using the orthogonality relationship. It is of the form $dE_k^{(n)}/dt = Q_k^{(n)} + C_k^{(n)} + R_k^{(n)} + (dE_k^{(n)}/dt)|_{\mathrm{NL}}$. As for the Fourier modes, $Q_k^{(n)}$ and $C_k^{(n)}$ represent the heat flux and dissipation terms of the nth POD mode, which are nonconservative, and $R_k^{(n)}$ is ignored as before. Calculating the time average of the sum of these two terms, we find that the first POD mode is unstable as it linearly inputs energy (positive $Q_k^{(1)} + C_k^{(1)}$) into the system. It has a mode structure very similar to the linearly unstable ITG mode [15]. The other modes ($n \geq 2$) are the subdominant modes, of which more than 99% are damped (negative $Q_k^{(n)} + C_k^{(n)}$). Nonlinear interactions of the POD modes are very similar to the Fourier mode triplets, $(dE_k^{(n)}/dt)|_{NL} = \sum_{k'} T_{k,k'}^{(n)}$, where $T_{k,k'}^{(n)}$ represents the three-wave interaction between the wave numbers k, k', and $k - k'$:

$$T_{k,k'}^{(n)} = \mathrm{Re}\Bigg\{ \int dz dv_{\parallel} d\mu \frac{\pi B_0 \hat{J} n_0 T_0}{F_0} (k' \times \hat{z} \cdot k)$$

$$\times [\beta_k^{(n)} \pi_k^{(n)} \psi_k^{(n)}]^* (g_{k'} \bar{\phi}_{k-k'} - \bar{\phi}_{k'} g_{k-k'}) \Bigg\}. \quad (3)$$

We look at the time-averaged and k_x'-summed spectrum of this nonlinear transfer, $\sum_{k_x'} \langle T_{k,k'}^{(n)} \rangle_t$, in Fig. 1. In Fig. 1(a), we see that the first POD mode at $k = (0, 0.25)$ couples primarily with $k_y' = 0.25$. This indicates a coupling with zonal modes because the third wave number in this triplet interaction has $k_y - k_y' = 0$. The sign of transfer is negative, with energy nonlinearly transferred out of the unstable POD mode. This exercise is repeated at zonal wave number $k = (0.1, 0)$, which has one of the highest zonal flow amplitudes. Figure 1(b) shows the net energy transfer spectrum of this wave number, summed over all POD modes. The positive transfer indicates that it receives energy nonlinearly and is linearly weakly damped. The peak of the energy transfer to this wave number is ~0.3 units, compared with the nonlinear transfer out of the unstable POD mode at $k = (0, 0.25)$ in Fig. 1(a), which is ~2 units. The zonal wave number $k = (0.1, 0)$ absorbs energy from many modes, of which $k = (0, 0.25)$ is only one; similarly, the unstable POD at $k = (0, 0.25)$ interacts with several zonal modes, of which $k = (0.1, 0)$ is only one. Nonetheless, we conclude that roughly one tenth of the energy coming out of the unstable mode at $k = (0, 0.25)$ is deposited into $k = (0.1, 0)$, of which the zonal flow is the dominant component. This is shown by a more thorough analysis below. As the energy is conserved, nine tenths of it should be deposited in the third mode in the three-wave interaction. Therefore, the zonal flow acts as a mediator of energy transfer: it is a component of the dominant energy transfer channel but absorbs only a small fraction of the steady-state transfer.

To which modes (unstable or subdominant) at the third wave number is this energy transferred? To answer this, we look at individual triplets and break them down into POD
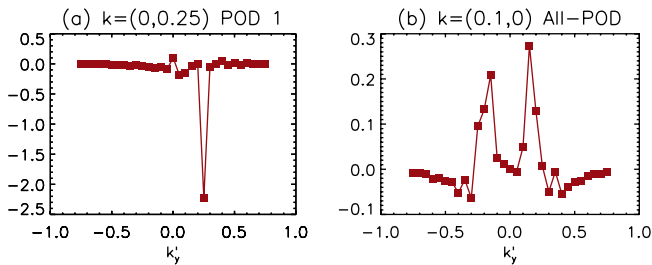
FIG. 1 (color online).   Time-averaged and k_x'-summed nonlinear transfer spectrum, $\sum_{k_x'} \langle T_{k,k'}^{(n)} \rangle_t$, as a function of k_y'. First 1000 POD modes are considered. (a) is for $n = 1$, $k = (0, 0.25)$; (b) is for sum over all $n = 1, 2, 3, \ldots, 1000$, $k = (0.1, 0)$. Positive values of $T_{k,k'}$ indicate energy flowing into mode k whereas negative values show energy flowing out of k.

modes (breaking all triplets into POD is computationally very expensive). It can be shown that energy is conserved in a triplet: $T_{k,k'}^{(1)} + T_{k,k'}^{(S)} + T_{k',k}^{(1)} + T_{k',k}^{(S)} + T_{k-k',k}^{(1)} + T_{k-k',k}^{(S)} = 0$. Here, S denotes all the subdominant modes summed together. $T_{k,k'}^{(1/S)}$ represents the energy transfer of the unstable or subdominant mode at k due to interaction with k' and $k - k'$. We select $k_y' = 0$ to make this a zonal mode triplet. Looking at these terms individually clearly shows the energy transfer occurring within a triplet.

We start by looking at $k = (0, 0.25)$, $k' = (0.1, 0)$, and $k - k' = (-0.1, 0.25)$. Its energy transfer terms are shown in block 1 of Fig. 2. The unstable mode at k transfers $T_{k,k'}^{(1)} = -119$ units of energy, summed over time in the saturated phase. By energy conservation, this is distributed amongst the other modes. Part goes into the higher-k unstable mode at $(-0.1, 0.25)$, $T_{k-k',k}^{(1)} = 66$, and part goes into the zonal mode, $T_{k',k}^{(1)} + T_{k',k}^{(S)} = 8$. As in Fig. 1(b), this is roughly one tenth of the energy input by the instability (119 units). The remainder of the energy goes to subdominant modes: $T_{k,k'}^{(S)} = 21$ units are absorbed at the original wave number k, while $T_{k-k',k}^{(S)} = 24$ units are taken up at $k - k'$. Of the 21 units, 15 go to the second POD mode at k, which is unstable, and 6 go to stable subdominant modes. Thus k injects $119 - 6 = 113$ units of energy into this triplet. Of this, 21% (24 units) is transferred to the damped subdominant modes at $k - k'$. In the subsequent blocks, all the subdominant modes at nonzonal wave numbers are damped. The percentages of energy transferred to damped subdominant modes in blocks 2, 3, 4, and 5 are 20%, 26%, 15%, and 27%, respectively. Combining the above percentages, 29% of the energy remains in the unstable modes at the end of block 5, while 71% has gone to damped subdominant modes. The energy transfer quantities in Fig. 2 are bispectral averages that require large ensembles to converge. Limited by computing time, we ran simulations with double the number of time steps to estimate that these quantities are uncertain within a factor of 2. However, the overall percentage of energy transferred to damped modes in the first five blocks remains large—92% in the longer simulation versus 71% in the shorter. This calculation was repeated for another set of triplets starting at $k = (0, 0.2)$ with the zonal wave number as $k' = (0.05, 0)$. By the end of block 5 at $k - k' = (-0.25, 0.2)$, the damped subdominant modes had absorbed 57% of the energy.

The data in Fig. 2 can be used to quantify the importance of dissipation by low-k damped modes compared to nonlinear energy transfer to high-k by constructing $R^{-1} = (k/T_k)(dT_k/dk)$ [17]. This dimensionless quantity is proportional at each k to the ratio of the rate of net energy dissipation, $\gamma_k E_k$, to the rate of conservative energy transfer, where γ_k is the difference of the linear instability
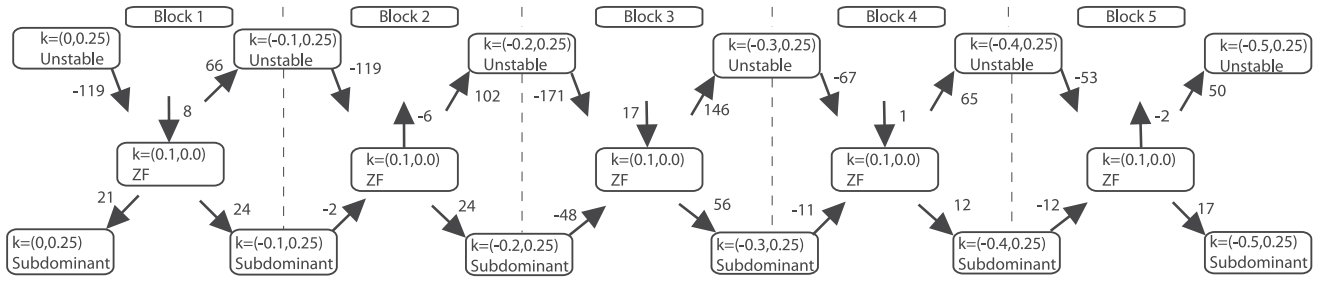
FIG. 2.   Energy transfer in three wave interactions, e.g., in block 1, $\sum_t T^{(n)}_{k,k'} = -119$ for $n = 1$, $k = (0, 0.25)$, and $k' = (0.1, 0)$. Similarly, in block 2, $\sum_{t,n} T^{(n)}_{k,k'} = 24$ for $n = 2, 3, \ldots$, $k = (-0.2, 0.25)$, and $k' = (-0.1, 0.25)$. See the text for discussion.

growth rate γ_{unst} and the net damping rate γ_{damp}, arising from the nonlinear excitation of damped modes. In Navier-Stokes turbulence R is equal to the Reynolds number at the outer scale and $R = 1$ at the Kolmogorov scale. From Fig. 2 four values of R are obtained from differences of T between blocks. These are $R^{-1} = 0.27$ for $k_x = -0.1$, $R^{-1} = 1.04$ for $k_x = -0.2$, $R^{-1} = -2.77$ for $k_x = -0.3$, and $R^{-1} = -0.64$ for $k_x = -0.4$. For $R < 0$, $\gamma_{\text{damp}} > \gamma_{\text{unst}}$ and vice versa. With $\gamma_k = \gamma_{\text{unst}} - \gamma_{\text{damp}}$, $|R^{-1}|$ is a *lower bound* on the quantity of interest to us, i.e., the ratio of stable mode energy absorption relative to energy transfer. Based on typical values of γ_{unst} and γ_{damp} for $k_x < 0.4$, this ratio is typically a factor of 3 larger than $|R^{-1}|$. We conclude that for $k_x < 0.4$, the energy absorption rate can be quite large (up to factor ~ 10) relative to the nonlinear energy transfer rate.

Figure 2 shows that the direction of energy transfer is from lower to higher radial wave numbers ("forward cascade"). The wave numbers in the figure do not lie in the high-k stable range conventionally associated with dissipation ($|k_x| \geq 0.5$ for $k_y = 0.25$). We calculate the ratio of net energy transfer to wave numbers within the unstable range to net transfer to wave numbers in the stable range for the first POD mode, $\sum_{k'} T^{(1)}_{k,k'}$. This is done for the nine wave numbers between $-0.05 \leq k_x \leq 0.05$ and $0.1 \leq k_y \leq 0.2$. Energy transfer is considered to be within the unstable range if the sum over k' is restricted to include only k' values with $|k'_x|$, $|k'_y|$, $|k_x - k'_x|$, $|k_y - k'_y| < 0.5$. Excluding these values from the sum gives the transfer to the stable range. The ratio of these two transfers for the nine wave numbers is around 4 on average, which indicates that for all the energy transferred to the high-k stable range, there is 4 times as much energy transfer to the unstable wave numbers. So while there is forward transfer, a large fraction of the injected energy is transferred to stable subdominant modes at low wave numbers before it reaches the conventional dissipation region.

The interaction of the unstable mode, zonal flow, and a subdominant mode dominates nonlinear transfer because of a combination of effects rooted in the three-wave correlation $\langle \pi^{(l)*}_k \pi^{(m)}_{k'} \pi^{(n)}_{k-k'} \rangle$, which governs the strength of transfer. From closure theory [18], $\langle \pi^{(l)*}_k \pi^{(m)}_{k'} \pi^{(n)}_{k-k'} \rangle = F[(|\pi|^2)^2] / (|\hat{\omega}^{(l)*}_k + \hat{\omega}^{(m)}_{k'} + \hat{\omega}^{(n)}_{k-k'}|)$, where F is a function of the

squared POD amplitudes $\pi^{(l,m,n)}$; l, m, and n are the POD numbers; and $\hat{\omega}^{(l,m,n)}$ are the nonlinear frequencies, estimated by fitting a Lorentzian to the frequency spectrum (see Ref. [19]). Figure 1 shows that triplets ($\langle \pi^{(l)*}_k \pi^{(m)}_{k'} \pi^{(n)}_{k-k'} \rangle$) that include a zonal mode are stronger relative to nonzonal triplets. Part of the reason is that the potential amplitude, π, at zonal modes is an order of magnitude higher than at nonzonal modes, whereas the situation is reversed when the zonal flows are suppressed. This higher amplitude leads to a higher F function for zonal mode triplets. Another part of the reason lies in the frequency sum, $|\hat{\omega}^{(l)*}_k + \hat{\omega}^{(m)}_{k'} + \hat{\omega}^{(n)}_{k-k'}|$, plotted in Fig. 3. We select $k = (0, 0.2)$, $k'_x = 0.1$ and scan over k'_y. At k the first POD mode is selected ($l = 1$), and m and n are varied over 1, 3, 5, 10, and 20. The average of these 5 combinations is also plotted. First, on average the minimum frequency sum is found at $k'_y = 0$, a zonal mode coupling, and $k'_y = 0.2$, also a zonal coupling, since $k_y - k'_y = 0$. Second, at both $k'_y = 0$ and $k'_y = 0.2$ the triplets with subdominant modes, i.e., $m = n = 3, 5, 10, 20$ show lower frequency sums than unstable mode triplets with $m, n = 1$. This shows that frequency matching is minimum between a triplet of unstable mode, zonal mode, and subdominant mode, thus maximizing energy transfer.
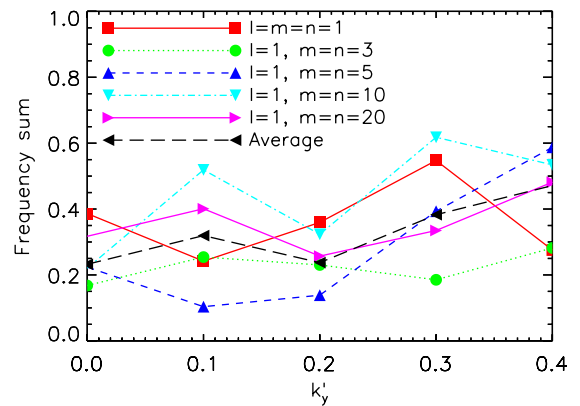
FIG. 3 (color online).   (Color online) Frequency sum, $|\hat{\omega}^{(l)*}_k + \hat{\omega}^{(m)}_{k'} + \hat{\omega}^{(n)}_{k-k'}|$, scanned over k'_y for $k = (0, 0.2)$, $k'_x = 0.1$.

We have shown that the energy injected by the instability strongly couples with the zonal flows and a stable mode. The zonal flows catalyze energy transfer to the subdominant modes, which are damped. The remainder is cascaded to higher radial wave numbers. At each stage of this cascade, a large fraction of the injected energy is transferred to damped subdominant modes that lie within the range of unstable wave numbers. This energy transfer to low-k damped modes can be several times the energy transfer to high-k modes. This is distinct from the shearing paradigm of zonal flows, which enhances conservative energy transfer to the high-k, stable range. It shows that coupling to subdominant modes cannot be ignored in the analysis of zonal-flow-regulated ITG turbulence.

---

[*]kirit.makwana@gmail.com

[1] J. W. Connor and H. R. Wilson, Plasma Phys. Controlled Fusion **36** 719 (1994).

[2] P. W. Terry, D. A. Baver, and S. Gupta, Phys. Plasmas **13**, 022307 (2006).

[3] K. D. Makwana, P. W. Terry, J.-H. Kim, and D. R. Hatch, Phys. Plasmas **18**, 012302 (2011).

[4] Z. Lin et al., Science **281**, 1835 (1998).

[5] G. W. Hammett M. A. Beer, W. Dorland, S. C. Cowley, and S. A. Smith, Plasma Phys. Controlled Fusion **35** 973 (1993).

[6] P. H. Diamond, S.-I. Itoh, K. Itoh, and T. S. Hahm, Plasma Phys. Controlled Fusion **47** (2005) R35.

[7] D. R. Hatch, P. W. Terry, W. M. Nevins, and W. Dorland, Phys. Plasmas **16**, 022311 (2009).

[8] K. D. Makwana, P. W. Terry, and J.-H. Kim, Phys. Plasmas **19**, 062310 (2012).

[9] A. J. Brizard and T. S. Hahm, Rev. Mod. Phys. **79**, 421 (2007).

[10] J. A. Krommes, Annu. Rev. Fluid Mech. **44**, 175 (2012).

[11] See http://gene.rzg.mpg.de for code details and access.

[12] M. J. Pueschel, T. Dannert, and F. Jenko, Comput. Phys. Commun. **181**, 1428 (2010).

[13] A. M. Dimits et al., Phys. Plasmas **7**, 969 (2000).

[14] A. B. Navarro, P. Morel, M. Albrecht-Marc, D. Carati, F. Merz, T. Görler, and F. Jenko, Phys. Plasmas **18**, 092303 (2011).

[15] D. R. Hatch, P. W. Terry, F. Jenko, F. Merz, M. J. Pueschel, W. M. Nevins, and E. Wang, Phys. Plasmas **18**, 055706 (2011).

[16] R. E. Waltz, and C. Holland, Phys. Plasmas **15**, 122503 (2008).

[17] P. W. Terry et al., Phys. Plasmas **19**, 055906 (2012).

[18] M. Lesieur, Turbulence in Fluids (Kluwer Academic Publishers, Dordrecht, Netherlands, 1990), pp. 161–175.

[19] P. W. Terry, and W. Horton, Phys. Fluids **26**, 106 (1983).